Modelling the impact of biogenic particle flux intensity and composition on sedimentary Pa/Th

Missiaen, Lise; Menviel, Laurie C.; Meissner, Katrin J.; Roche, Didier M.; Dutay, Jean Claude; Bouttes, Nathaelle; Lhardy, Fanny; Quiquet, Aurélien; Pichat, Sylvain; Waelbroeck, Claire

published in
Quaternary Science Reviews
2020

DOI (link to publisher)
10.1016/j.quascirev.2020.106394

document version
Publisher's PDF, also known as Version of record

Quaternary Science Reviews 240 (2020) 106394

Contents lists available at ScienceDirect

Quaternary Science Reviews

journal homepage: www.elsevier.com/locate/quascirev

Modelling the impact of biogenic particle flux intensity and composition on sedimentary Pa/Th

Lise Missiaen [a, *], Laurie C. Menviel [a], Katrin J. Meissner [a, b], Didier M. Roche [c, d], Jean-Claude Dutay [c], Nathaelle Bouttes [c], Fanny Lhardy [c], Aurélien Quiquet [c, e], Sylvain Pichat [f, g], Claire Waelbroeck [h]

[a] Climate Change Research Centre, University of New South Wales, Sydney, Australia
[b] ARC Centre of Excellence for Climate Extremes, University of New South Wales, Sydney, Australia
[c] Laboratoire des Sciences du Climat et de l'environnement, LSCE/IPSL, CEA-CNRS-UVSQ-Université Paris Saclay, F91-198, Gif sur Yvette, France
[d] Vrije Universiteit Amsterdam, Faculty of Science, Cluster Earth and Climate, de Boelelaan 1085, 1081, HV, Amsterdam, the Netherlands
[e] Institut Louis Bachelier, Chair Energy and Prosperity, Paris, 75002, France
[f] Univ Lyon, ENSL, Univ Lyon 1, CNRS, LGL-TPE, F-69007, Lyon, France
[g] Max Planck Inst Chem, Climate Geochem Dept, Hahn Meitner Weg 1, D-55128, Mainz, Germany
[h] LOCEAN/IPSL, Sorbonne Université-CNRS-IRD-MNHN, UMR7159, Paris, France

ARTICLE INFO

Article history:
Received 23 October 2019
Received in revised form
29 May 2020
Accepted 29 May 2020
Available online 19 June 2020

Keywords:
Ocean circulation
Particle fluxes
Pa/Th
Abrupt climate events

ABSTRACT

There is compelling evidence that millennial climate variability of the last glacial period was associated with significant changes in the Atlantic Meridional Overturning Circulation (AMOC). Several North Atlantic sedimentary Pa/Th records indicate a consistent and large Pa/Th increase across millennial-scale events, which has been interpreted as considerable reduction in North Atlantic Deep Water (NADW) formation. However, the use of sedimentary Pa/Th as a pure kinematic circulation proxy is challenging because Pa and Th are also highly sensitive to changes in particulate flux intensity and composition that might have occurred across these millennial scale events. In this study, we use the Pa/Th enabled iLOVECLIM Earth System Model of intermediate complexity to evaluate the impact of changes in biogenic particle flux intensity and composition on the Atlantic Pa/Th. We find that in our model, changes in Particulate Organic Carbon (POC), and to a lesser extent biogenic opal production, can significantly affect the sedimentary Pa/Th, possibly explaining up to 30% of the observed North Atlantic Pa/Th increase across Heinrich stadial 1. The sedimentary Pa/Th response is also likely sensitive to shifts in the geographical distribution of the particles, especially in high scavenging regions. Our study suggests that a decrease in opal production in the northwest Atlantic can induce a far field Pa/Th increase in a large part of the North Atlantic basin. Therefore, local monitoring of particle fluxes may not be sufficient to rule out any influence of changing particle fluxes on sedimentary Pa/Th records.

1. Introduction

There is compelling evidence that the millennial-scale climate variability of the last glacial period was associated with significant changes in the Atlantic Meridional Overturning Circulation (AMOC) (see (Lynch-Stieglitz, 2017) for a review). The most prominent millennial scale climate events are Heinrich stadials, which correspond to cold North Atlantic periods associated with massive iceberg discharges (see (Hemming, 2004) for a review). The most widely accepted hypothesis to account for the North Atlantic cooling during those stadials involves a reduced poleward heat transport caused by a weakening or shutdown of the AMOC (e.g. (Rahmstorf, 2002)).

Among available proxies, one of the most valuable to reconstruct past changes in AMOC strength is the ($^{231}Pa_{xs,0}/^{230}Th_{xs,0}$), which corresponds to the activity ratio of ^{231}Pa (Pa hereafter) and ^{230}Th (Th hereafter) derived from water column scavenging (subscript "xs") at the time of the deposition (subscript "0") - hereafter simply noted Pa/Th. The two isotopes are produced homogeneously in the water column by decay of their parent U

* Corresponding author.
E-mail address: l.missiaen@unsw.edu.au (L. Missiaen).

https://doi.org/10.1016/j.quascirev.2020.106394
0277-3791/

isotopes at a known and constant ratio, called the production ratio, which is equal to 0.093 (dpm/dpm). The dominant ocean sink of Pa and Th is particle scavenging, while radioactive decay plays a smaller role due to their relatively long half-lives (32 760 years for Pa and 75 380 years for Th). As Pa and Th have distinct particle reactivities, and thus different residence times in the water column, the oceanic circulation can influence the sedimentary Pa/Th ratio. Th is more rapidly scavenged and transferred to the sediments than Pa because of its higher particulate reactivity. Hence, its residence time in the water column (10–40 years (Henderson and Anderson, 2003),) is shorter than that of Pa (50–200 years). Therefore, Pa can be transported further by ocean circulation than Th. It is estimated that about 26% of the Pa (and only 4% of the Th) produced in the North Atlantic is transported southwards, out of the Atlantic basin, in the modern ocean (Deng et al., 2018). The excess Pa is transferred to the sediments in the Southern Ocean, rich in opal, which is known to be a strong scavenger for Pa (Chase et al., 2002; Walter et al., 1997). The sedimentary Pa/Th in North Atlantic cores is therefore lower than the production ratio and any increase towards the production ratio results for a large part from a reduction in southward Pa advection by the AMOC. The use of Pa/Th as a kinematic circulation proxy only holds for the Atlantic basin where Pa transport by ocean circulation is dominant over particle-related Pa transport across the particle flux gradients.

A recent Pa/Th compilation over the last deglaciation (Ng et al., 2018) showed a consistent Pa/Th increase of roughly 0.03 Pa/Th units in the North Atlantic during Heinrich stadial 1 (McManus et al., 2004; Mulitza et al., 2017; Ng et al., 2018). This has been interpreted as an indication of a possible complete AMOC shutdown (off-mode).

However, the use of Pa/Th as a kinematic circulation proxy has been debated (e.g. (Lippold et al., 2012b, 2011, 2009), on the basis that the Pa/Th ratio is not only controlled by circulation strength but also by particle scavenging. Pa and Th scavenging efficiencies and affinities for different sediment components have been intensively studied (e.g. (Chase et al., 2003, 2002; Luo and Ku, 2004, 1999)), recently taking advantage of the GEOTRACES water column database (Hayes et al., 2015b). It has been shown that changes in the particle flux intensity and/or composition can significantly increase or decrease the residence time of Pa, and to a lesser extent that of Th (Chase et al., 2003, 2002; Luo and Ku, 2004). As a consequence, Pa and Th can be transported from low particle flux or low scavenging areas to high particle flux and/or high scavenging areas (across the particle fluxes gradients), which is usually referred to as the boundary scavenging effect (Anderson et al., 1983; François, 2007) and can ultimately modify the sedimentary Pa/Th ratio.

Even if quantitative estimates are still lacking, substantial changes in marine productivity and subsequent changes in both particle composition and flux intensity have been evidenced across the millennial-scale events of the last glacial, from both paleo data (e.g. (Cartapanis et al., 2018, 2016; Kienast et al., 2016)) and modelling studies (e.g. (Mariotti et al., 2012; Menviel et al., 2008; Schmittner, 2005). It has also been proposed that a switch in predominant plankton types from diatom-dominated assemblages (i.e. opal producers) to coccolithophore-dominated assemblages (i.e. $CaCO_3$ producers) could have occurred at low latitudes in relation to changes in the environmental conditions (Brzezinski et al., 2002; Matsumoto et al., 2002). The impact of particle composition on the paleo Pa/Th records has been previously assessed indirectly by analyzing the sediment composition (e.g. (Böhm et al., 2015; Gherardi et al., 2009; Lippold et al., 2012a). These analyses mostly focused on the evolution of the sedimentary opal content as opal is known to strongly affect Pa scavenging. A few recent studies also assessed the evolution of the detrital particle flux and its impact on sedimentary Pa/Th (Burckel et al., 2015; Missiaen et al., 2018; Waelbroeck et al., 2018). Generally, the Pa/Th signal has been considered to be mainly driven by circulation changes if 1) the reconstructed sedimentary opal fluxes are lower than an empirical threshold deduced from observations (see (Lippold et al., 2012a)), and/or 2) there is no significant correlation between the reconstructed particle fluxes and the Pa/Th over the considered time period (e.g. (Böhm et al., 2015; Burckel et al., 2015; Waelbroeck et al., 2018). This approach has several major limitations: 1) the sediment content only represents the preserved particles, which may differ significantly from the export particle production at the deposition time due to changes in remineralization intensity (e.g. (Dunne et al., 2007)) or postdeposition dissolution (Farrell and Prell, 1989; Le and Shackleton, 1992; Richaud et al., 2007; Stephens and Kadko, 1997); 2) only the impact of opal fluxes variations has been systematically investigated although Pa and Th are transferred to the sediments by at least 3 other particles types (POC, $CaCO_3$ and lithogenic); 3) though it has been acknowledged that strong particle flux gradients can induce Pa and Th transport across sub-basins (also called « boundary scavenging » (François, 2007)), the particle composition and flux intensity evolutions have been investigated at the considered core sites only, without taking into account any influence of neighboring or regional productivity changes. The latter could indeed induce changes in Pa or Th concentrations at the considered core site location and therefore bias the sedimentary Pa/Th circulation signal. Such biases have been predicted in theory (François, 2007) and references therein) and confirmed by sensitivity experiments in modelling studies (e.g. (Lippold et al., 2012a; Luo et al., 2010).

Because Pa/Th is a complex but valuable proxy of circulation strength, Pa and Th scavenging has been included into several models of varying complexity over the last decades, with the aim to better understand its behavior. The simplest versions consist in 1D box models (e.g. (Nozaki et al., 1981; Roy-Barman, 2009) and zonally averaged 2D models (Luo et al., 2010; Marchal et al., 2000). More complex studies include a 3D set-up in coarse resolution models (Henderson et al., 1999) and with simplified particle representation (Siddall et al., 2007, 2005). The latest developments consider more sophisticated and interactive particle representations in state-of-the-art climate models (Gu and Liu, 2017; van Hulten et al., 2018), and models of intermediate complexity (Missiaen et al., 2020; Rempfer et al., 2017). Some models also include parametrizations to account for the impact of high magnitude coastal fluxes and bottom sediment remobilization on Pa and Th scavenging (Rempfer et al., 2017). These models offer the opportunity to improve our understanding of Pa and Th behavior with respect to circulation and particle changes. To date, some sensitivity experiments have been performed to investigate the impact of the equilibrium partition coefficient (e.g. (Gu and Liu, 2017; Siddall et al., 2005; van Hulten et al., 2018) and circulation changes (Gu and Liu, 2017; Missiaen et al., 2020; Rempfer et al., 2017; Siddall et al., 2007) but little has been done to investigate the impact of changes in particle flux intensity and composition on the sedimentary Pa/Th ratio with a 3D model. While (Lippold et al., 2012a; Luo et al., 2010) tested the impact of particle flux changes in a 2D model framework (Siddall et al., 2007), described the impact of halving and minimizing the total particle fluxes (POC, $CaCO_3$ and opal) in a hosing experiment with a focus on the North Atlantic. To date there has been no comprehensive study assessing the impact of changes in individual particle composition and fluxes.

In this study, we use the Earth System model of intermediate complexity iLOVECLIM to 1) better constrain the role of biogenic particles on sedimentary Pa/Th ratio in a 3D perspective and 2)

assess the potential impact of large-scale past changes in global particle fluxes on paleo Pa/Th records.

2. Methods

2.1. iLOVECLIM Pa/Th module

We use the Earth System model of intermediate complexity iLOVECLIM, which is a fork development of the LOVECLIM model (Goosse et al., 2010). iLOVECLIM includes modules representing the atmosphere (ECBilt), the ocean (CLIO), the sea ice, and the land vegetation (VECODE). The ocean component (CLIO) consists of a free-surface primitive equation ocean model with a resolution of 3° × 3° (corresponding to 120 longitudinal and 65 latitudinal grid cells) and 20 depth layers. A module computing the evolution of dissolved and particulate ^{230}Th and ^{231}Pa in the ocean has been recently added and is fully described in (Missiaen et al., 2020). This Pa/Th module explicitly computes the input of Pa and Th from U decay, their radioactive decay, and their removal by particle scavenging (i.e. adsorption/desorption and particle settling) following the Bacon and Anderson reversible scavenging model (Bacon and Anderson, 1982). In line with other modelling studies (Gu and Liu, 2017; Rempfer et al., 2017) and for simplicity, we have only considered biogenic particles in this study. Nevertheless, the lithogenic particles have been found to have high scavenging efficiencies on Pa and Th (Hayes et al., 2015b), and to potentially represent a significant amount of the total particle fluxes (Conte et al., 2001), or to form nepheloid layers that affect the Pa and Th behavior at the bottom of the oceans (Costa et al., 2020), and would therefore deserve to be considered in future studies. We consider a single particle size class and three different biogenic particle types: biogenic opal, particulate organic carbon (POC), and calcium carbonate ($CaCO_3$). Like in other Pa/Th models (Gu and Liu, 2017; Rempfer et al., 2017; Siddall et al., 2007, 2005), the particles are given a uniform settling speed of 1000 m/y, in agreement with previous estimations (Anderson et al., 2016; Gdaniec et al., 2018; Krishnaswami et al., 1976). The Pa/Th module is not coupled to iLOVECLIM's biogeochemical model because iLOVECLIM does not simulate the oceanic Si cycle. The Pa/Th module therefore does not use prognostic particle fluxes in this study. Instead, the model uses prescribed and fixed 3D particle fields obtained from a preindustrial simulation with the Ocean General Circulation Model (OGCM) NEMO-PISCES. These fields have been described and validated against observations. In particular, it has been acknowledged that while the $CaCO_3$ and POC concentrations are generally underestimated, the opal concentrations are overestimated, in particular on the western margin along the American coast (see (van Hulten et al., 2018) for details). iLOVECLIM computes the transport (advection and diffusion) of the four tracers (i.e. the dissolved and particulate Pa and Th). The scavenging coefficients used in iLOVECLIM are presented in Table 1 and are discussed in more detail in (Missiaen et al., 2020). The simulated dissolved and particulate Pa and Th patterns as well as sedimentary Pa/Th have been evaluated against the recent GEOTRACES observations (Deng et al., 2014; Hayes et al., 2015a, 2015b) and a core-top compilation (see (van Hulten et al., 2018) and references therein). The model performance in simulating the water column and sedimentary Pa and Th is comparable to state-of-the-art ocean circulation models (see (Missiaen et al., 2020). Our model is computationally efficient, able to simulate 800 years of Pa and Th evolution in about 24 h.

$$Kd_{(i,j)} = \frac{\sigma_{i,j} \times w^s \times \rho_{sw}}{M^{(i)} \times k^{desorp}}$$

where $Kd_{(i,j)}$ is the partition coefficient for isotope i (Pa or Th) for particle type j (POC, $CaCO_3$ or opal), $\sigma_{i,j}$ are the scavenging efficiencies for isotope i of particle j that are obtained after model optimization as described in (Missiaen et al., 2020), w^s is the settling speed, K^{desorp} is the desorption coefficient considered constant and equal to 2.4 y^{-1}, $M^{(i)}$ is the molar mass of particle type i (i.e. 12 g mol^{-1} for POC, 100.08 g mol^{-1} for $CaCO_3$ and 67.3 g mol^{-1} for opal) and ρ_{sw} is the mean density of sea water (constant and fixed to 1.03 10^6 g m^{-3}).

2.2. Experimental design

The model was first equilibrated for 5000 years (control run) under PI boundary conditions with control particle fields as described in (Missiaen et al., 2020; van Hulten et al., 2018). In order to investigate the potential impact of large-scale changes in particle flux intensity and composition on the sedimentary Pa/Th, we perform ten idealized sensitivity experiments in which we vary the prescribed particle fields under pre-industrial (PI) boundary conditions (Table 2). The idealized sensitivity experiments are run for 1000 years each, and the particle flux fields (i.e. concentration times settling speed) are globally increased or decreased by multiplying the particle concentrations by a fixed factor (i.e. preserving the regional patterns of the PI control particles, and keeping the settling speed constant) as described in Table 2. The particle forcing is shown in Fig. 1. Given that the residence time of Pa and Th in the ocean have been estimated to be about 200 and 40 years respectively (Henderson and Anderson, 2003), the duration of our

Table 2
Particle flux forcing applied in sensitivity experiments under PI boundary conditions. The particle fluxes have been altered globally by changing the particle concentration, keeping the settling speed at 1000 m/y. Twice the PI flux is denoted CTRLx2, half the PI flux is denoted CTRL_2.

Simulation name	POC	$CaCO_3$	Opal
CTRL	CTRL	CTRL	CTRL
All_x2	CTRL x2	CTRL x2	CTRL x2
All_2	CTRL/2	CTRL/2	CTRL/2
Opal_x2	CTRL	CTRL	CTRL x2
Opal_2	CTRL	CTRL	CTRL/2
CaCO3_x2	CTRL	CTRL x2	CTRL
CaCO3_2	CTRL	CTRL/2	CTRL
POC_x2	CTRL x2	CTRL	CTRL
POC_2	CTRL/2	CTRL	CTRL
Opal_2_CaCO3_x2	CTRL	CTRL x2	CTRL/2

Table 1
Scavenging coefficients in iLOVECLIM.

a) Sigma coefficients (as parametrized in iLOVECLIM)					
σ_Pa_CaCO3	σ_Pa_POC	σ_Pa_opal	σ_Th_CaCO3	σ_Th_POC	σ_Th_opal
1.87	1.55	7.62	76.83	5.47	3.77
b) Kd equivalents (see (Missiaen et al., 2020))					
Kd_Pa_CaCO3	Kd_Pa_POC	Kd_Pa_opal	Kd_Th_CaCO3	Kd_Th_POC	Kd_Th_opal
8.01 E+06	5.53 E+07	4.86 E+07	3.29 E+08	1.96 E+08	2.40 E+07

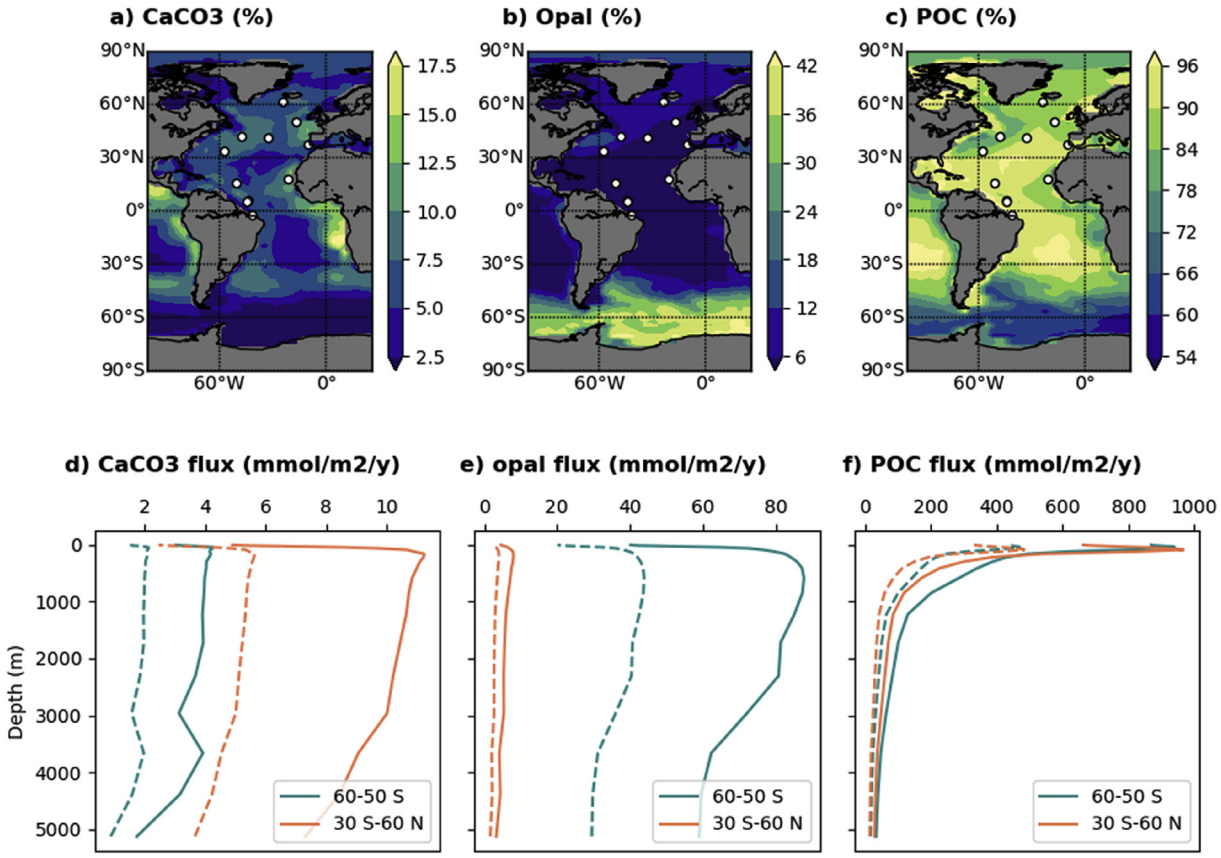

Fig. 1. Particle forcing. Percentage of each particle type obtained by integrating the considered particle concentrations over the water column and normalizing by the sum of the integrated concentrations of all particles ($CaCO_3$ + opal + POC = 100%) for each grid-cell for a) $CaCO_3$, b) opal and c) POC. All particle fields used in this study are derived from a preindustrial simulation performed with NEMO-PISCES (van Hulten et al., 2018) (see methods). The white dots represent the locations of cores with available Pa/Th time series covering Heinrich stadial 1 (Ng et al., 2018). Zonally averaged Atlantic particle profiles expressed as particle fluxes (mmol/m^2/y) for d) $CaCO_3$, e) opal and f) POC. The blue lines represent the average profile between 50°S and 60°S, the orange lines represent the average profile between 30°S and 60°N. The dashed lines represent the particle forcing profiles for halved concentrations. The export particle fluxes at 75 m are presented in Figure S1.

sensitivity simulations is sufficient to reach equilibrium as shown in previous studies (Missiaen et al., 2020; van Hulten et al., 2018). We then compare the last 100 years of each simulation with 100 years of the PI control simulation.

It has been suggested that changes in environmental conditions during episodes of past climate change (such as the last deglaciation) might have triggered a switch between dominant plankton assemblages (namely between diatoms that produce biogenic silica and coccolithophores that mostly produce $CaCO_3$ (Brzezinski et al., 2002; Matsumoto et al., 2002)). The hypothesis states that silicic acid might have been transported towards lower latitudes where it would have enhanced diatom productivity under glacial conditions, knowing that silicic acid availability is a limiting nutrient at low latitudes today. During the last deglaciation, the diatom productivity might therefore have decreased at low latitudes, while the coccolithophore productivity might have increased, as a result of changes in temperature as well as nutrient (and in particular Si) availability. This might have changed the water column $CaCO_3$/opal rain ratio, consistent with large marine ecosystem reorganizations across climatic transitions suggested by modelling studies (e.g. (Bopp et al., 2005; Marinov et al., 2010)). In addition, lower $CaCO_3$ burial rates despite higher sediment accumulation rates (105% of the Holocene mass accumulation rate) have been reported during the Last Glacial Maximum (LGM) (Cartapanis et al., 2018). Although post depositional dissolution cannot be excluded, these results are consistent with reduced coccolithophore production at the LGM. Here, we test the impact of such plankton assemblage changes by globally increasing the $CaCO_3$ concentrations and decreasing the opal concentrations by a factor of 2 assuming that the total productivity (POC) concentration remained constant.

The Pa and Th fluxes to the sediment presented in this study correspond to the Pa or Th activity in the bottom ocean grid cell (deepest flooded grid cell) multiplied by the uniform particle settling speed of 1000 m/y.

Under PI boundary conditions, the simulated AMOC in iLOVECLIM is about 17 Sv with interannual and decadal variability of ± 2 Sv. To account for this variability, we tested the significance of the changes due to particle modifications as follows. We define the natural variability of the sedimentary Pa/Th as its variance (2 sigma) evaluated over the last 100 years of the PI control simulation. Then, we evaluate the significance of the anomaly between the average sedimentary Pa/Th in a perturbed simulation and in the control run over the 100 final years of the simulation. An anomaly is considered to be significant if it exceeds the natural variability (i.e. anomaly >4 sigma).

3. Results

3.1. Pa and Th scavenging in iLOVECLIM under control PI conditions

Before analyzing the impact of changes in particle flux intensity and composition, we start by describing the scavenging of Pa and

Th in the control PI run. We define the normalized Pa and Th flux to the sediments as the ratio of the Pa and Th buried in the sediments to the local production in the overlying water column. In the absence of any Pa or Th transport, the Pa and Th burial would equal the production in the corresponding overlying water column. Therefore, when the normalized fluxes are different from 1, they indicate the extent of Pa and Th transport in the Atlantic either related to the deep circulation or to the particle gradients (Fig. 2). The normalized flux to the sediments ranges between 0.5 and 1.4 for Th (median = 1 (as expected), 1 sigma = 0.34) while it ranges between 0.3 and >2 for Pa (median = 1 (as expected), 1 sigma = 0.76), highlighting that a larger proportion of the Pa is transported within the Atlantic basin compared to Th. The simulated normalized Pa and Th fluxes display a common geographical pattern. The two isotopes are preferentially buried in the sediments along the North American continental margin (between 30°N and 50°N), off the Argentinian coast (between 20°S and 60°S) and off the African coast. Pa is also effectively buried in the Southern Ocean opal belt (between 40°S and 60°S), which is consistent with the transport of Pa from the North Atlantic to the Southern Ocean by the AMOC (Walter et al., 1997). The two isotopes also tend to be transported away from the basin interior (i.e. in the two subtropical gyres - ~10°N to 40°N and ~10°S to 40°S)).

Overall, the regions of effective Pa and Th burial correspond to regions where marine productivity is active and produces large fluxes of biogenic particles (Fig. 2 - Figure S1). In such regions, dissolved Pa and Th are rapidly adsorbed onto the particles because of the high particle fluxes and are actively transferred to the sediments. Consistently, there is a deficit of dissolved Pa and Th, which is dynamically altered by eddy advection and diffusion.

3.2. Impact of globally uniform changes in particle fluxes

In this section we describe the impact of globally uniform changes in particle fluxes on Pa and Th scavenging under PI boundary conditions (see methods). As we obtain quasi symmetric responses for the doubling and halving of particle concentrations, we only discuss the case of reduced particle concentrations. The results of experiments where particle concentrations were doubled are shown in the supporting information (Figures S2, S3 and S5).

3.2.1. Dissolved Pa and Th

Although dissolved Pa and Th activities (hereafter simply designated by dissolved Pa and Th) are not accessible in the paleorecords, their spatial distribution provides insights into the particle type that most effectively scavenges Pa and Th to the sediments in different sub-regions of the Atlantic basin.

As expected, a decrease in the total particle flux (all_2) leads to an increase in dissolved Pa and Th across the entire Atlantic basin, because less Pa and Th is being scavenged and removed from the water column by particles (Fig. 3). In our model, halving the particle content in the whole water column roughly doubles the dissolved Pa and Th activities, suggesting a quasi linear response of the dissolved phase (Fig. 3). The magnitude of the changes in dissolved Pa and Th is sensitive to the type of the altered particles, consistent with the prescribed scavenging affinities (Table 1). Halving POC concentrations (POC_2) increases both the dissolved Pa and Th by ~40% in most of the Atlantic basin. By contrast, changing the opal or $CaCO_3$ concentrations creates region specific responses. Halving the opal concentration (opal_2) results in a 80% increase in dissolved Pa in the Southern Ocean while dissolved Th is increased by ~15% in the Southern Ocean and displays no significant change in the rest of the basin. Finally, halving the $CaCO_3$ concentrations (CaCO3_2) leads to a 15% increase in dissolved Pa and a 50–60% increase in dissolved Th concentrations in most of the Atlantic Ocean (Fig. 3).

We note that $CaCO_3$ and POC are mostly present north of 40°S, with POC being the most abundant particle (Fig. 1). In the Southern Ocean, opal is the most abundant particle while POC and $CaCO_3$ have very low concentrations. The geographical pattern of dissolved Pa and Th variations is closely correlated to particle distribution: the highest changes in dissolved Pa and Th are observed in high particle flux regions such as coastal areas and the Southern Ocean opal belt (i.e. high scavenging intensity regions, see Section 3.1). Halving POC or $CaCO_3$ concentrations leads to an increase in dissolved Pa north 40°S, while halving opal concentrations increases the dissolved Pa in the Southern Ocean and to a lesser extent along the North American coastal margin (between 30°N and 50°N) (Fig. 3). By contrast, decreasing $CaCO_3$ concentrations increases the dissolved Th north of 40°S while decreasing the opal or POC concentrations increases the dissolved Th in the Southern Ocean (Fig. 3).

Our simulations highlight that in our model Pa is mostly

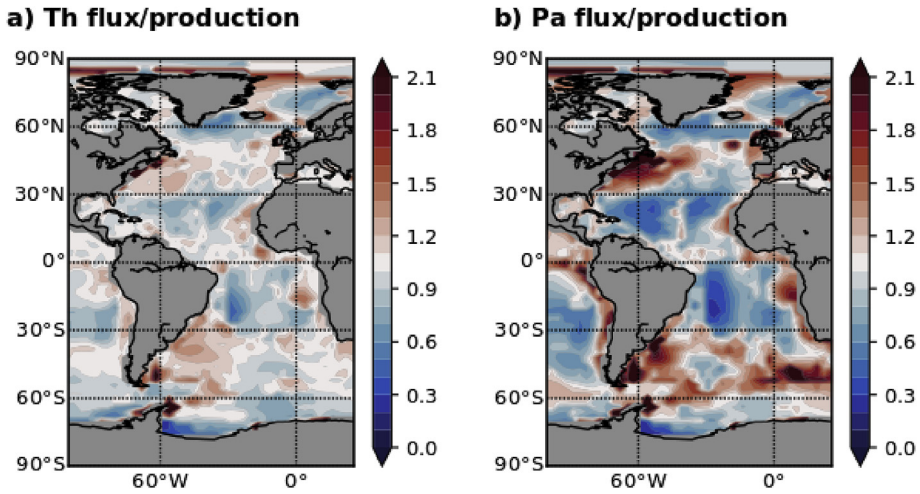

Fig. 2. Pa and Th flux to the sediments normalized to the production in the overlying water column. a) Th flux/production b) Pa flux/Production i.e. ratio between the Pa or flux to the sediment and the production in the overlying water column calculated in each grid cell. Values lower than 1 indicate that Pa and/or Th have been transported away. The areas of high Pa and Th fluxes, in particular along the coast of North America (between ~30°N and 50°N), South America (~30°S –60°S) and the African coast, correspond to regions of high particle fluxes (see Fig. 1).

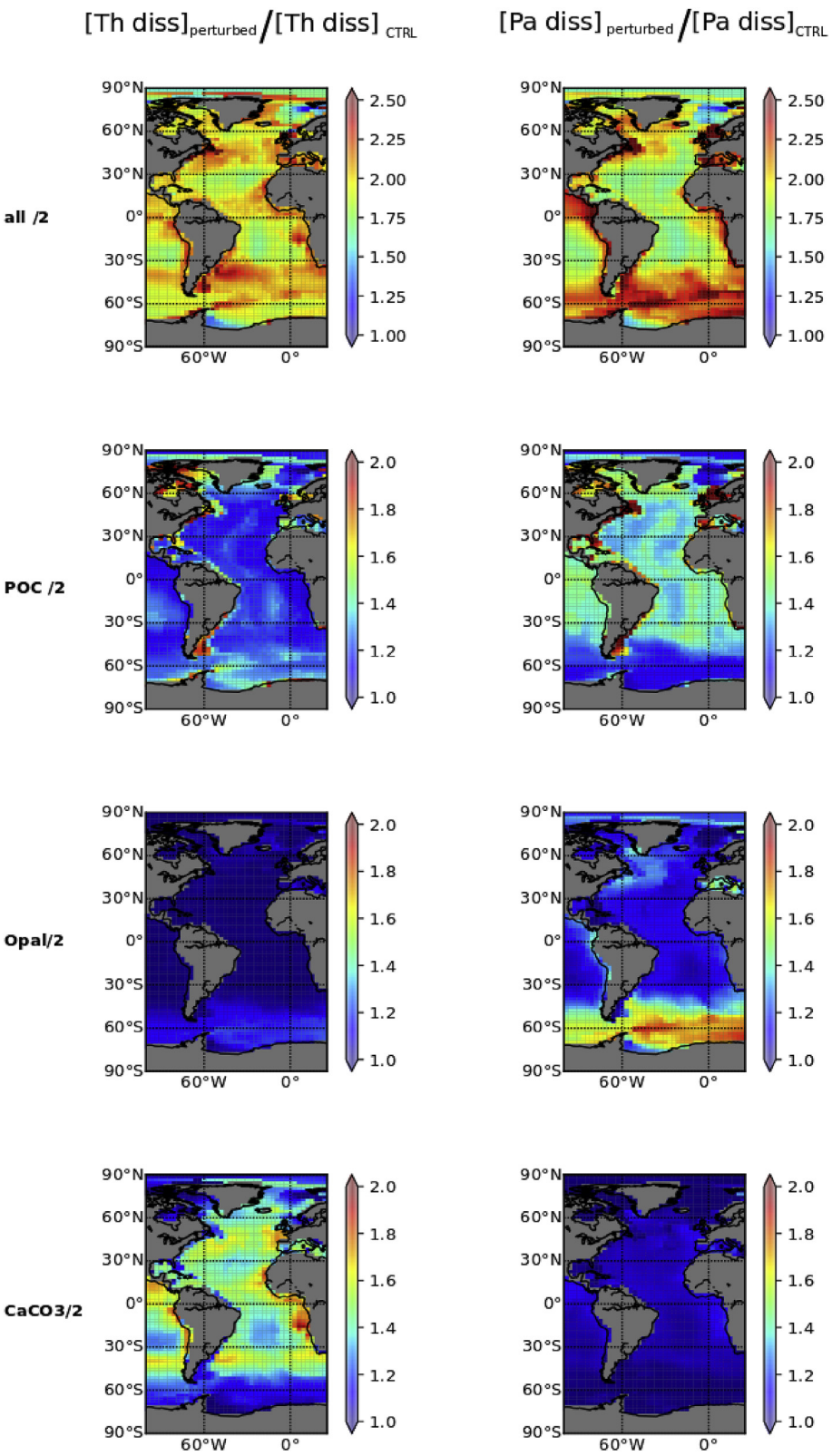

Fig. 3. Ratio between water column integrated dissolved Th and Pa activities ([Pa diss] and [Th diss]) of the corresponding perturbed simulations and the equivalent from the PI control simulation (CTRL). Values equal to 1 indicate no change, values > 1 indicate more dissolved Pa and Th.

transferred to the sediments by opal in the Southern Ocean as well as off the North American coast (between 30°N and 50°N) where our prescribed particle fields contain a relatively high amount of opal. Elsewhere, Pa is transferred to the sediments by POC and to a lesser extent by $CaCO_3$. Th is the element that is most effectively transferred to the sediments by $CaCO_3$ in most of the Atlantic basin. In the Southern Ocean, where there is less $CaCO_3$, Th is scavenged by opal and POC with roughly the same efficiency. This is consistent with the prescribed affinities of Pa and Th for the different particle types (Table 1).

3.2.2. Sedimentary Pa/Th

In this section, we focus our analysis on the modelled sedimentary Pa/Th, which corresponds in our simulations to the ratio of the particulate Pa and Th in the deepest ocean grid cell (see methods). We note that the spatial pattern of sedimentary Pa/Th response is comparable to the spatial pattern of sedimentary Pa (Figures S4 and S5), highlighting the driving role of Pa in the sedimentary Pa/Th response. Contrarily to what we observed for dissolved activities, halving the particle fluxes does not produce a uniform Pa/Th change throughout the whole Atlantic. Instead, the Pa/Th response to particle changes has an interesting geographical pattern that we describe below for our different simulations (all_2, opal_2, CaCO3_2 and POC_2). The results of the simulations in which we multiply the particle fields by 2 are presented in the supplementary material (Figure S3).

Decreasing the total particle concentration (all_2) decreases the sedimentary Pa/Th by about 0.016 in most of the Atlantic basin (Fig. 4). The magnitude of the Pa/Th decrease in coastal regions is about twice as large as in the basin interior. In the Southern Ocean and along the West African coast, decreasing the total particle concentration induces a Pa/Th increase of 0.012–0.02 (Fig. 4). In this simulation, less Pa is transferred to the sediments in the Atlantic basin, leaving more Pa to be transported into the Southern Ocean, where it is scavenged by opal. The same overall sedimentary Pa/Th pattern is observed in the POC_2 experiment, with anomalies of slightly lower amplitude: the Pa/Th decreases by about 0.012 in the major part of the Atlantic basin and increases by about 0.01–0.018 in the South Atlantic, off the West African coast and off the North American coast (between 30°N and 50°N). These changes show that in our simulations POC is the main scavenger particle type for Pa, except south of 40°S, in the Southern Ocean opal belt. Interestingly, according to the scavenging coefficients (Table 1), Pa affinity for POC is not particularly high, especially when compared to its affinity for opal (i.e. Kd_Pa_POC is almost equal to Kd_Pa_opal). But the scavenging intensity is driven by both the affinity and the particle flux (i.e. particle concentration multiplied by the settling speed). The high POC fluxes, which are 12–35 times higher than the opal and $CaCO_3$ fluxes (Fig. 1) in the Atlantic basin north of 40°S, explain the high sensitivity of Pa to changes in POC concentrations. Looking at the POC profiles (Fig. 1), we note that the high concentrations are restricted to the first 300 m and rapidly decrease with depth. Our model therefore suggests that surface productivity changes can significantly affect deep/sedimentary Pa/Th, highlighting the role of POC to effectively transfer the Pa produced in the upper water column to deeper layers.

Though opal is only abundant in the Southern Ocean, a decrease in opal concentration (opal_2) also produces significant sedimentary Pa/Th changes with a slightly more complex geographical pattern. The sedimentary Pa/Th decreases by 0.012–0.02 in the South Atlantic (around 40°S) and off the North American coast (between 30°N and 50°N). There is a minor decrease (around 0.008) along the equator between 10°S and 10°N. Elsewhere, and in particular in the two subtropical gyres, which are depleted in opal, the Pa/Th increases by about 0.01 (Fig. 4).

Finally, halving the $CaCO_3$ concentrations (CaCO3_2) has the least impact on sedimentary Pa/Th (<0.0008), with Pa/Th increasing in the subtropical gyres and decreasing elsewhere. The

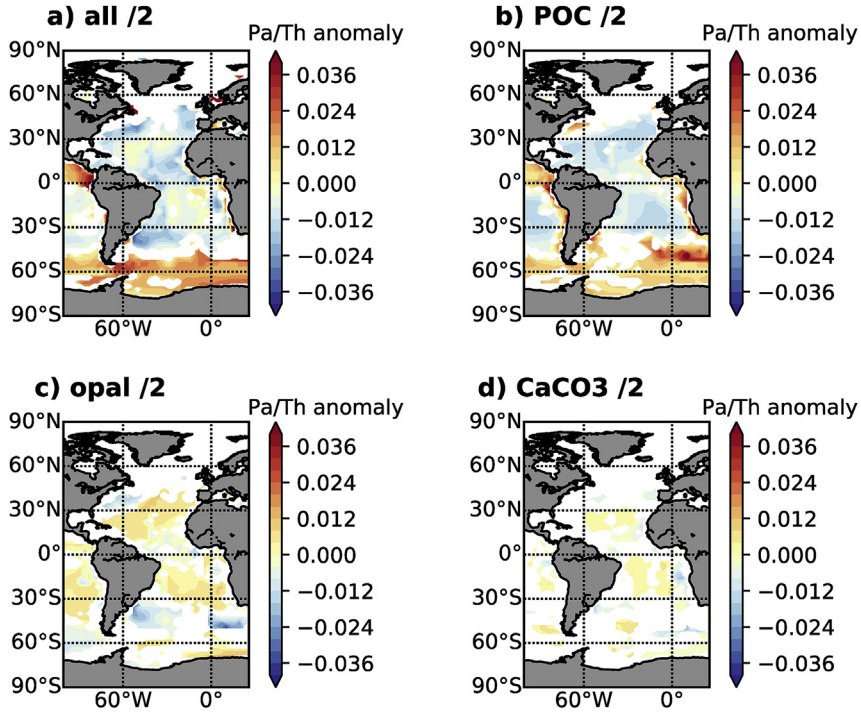

Fig. 4. Sedimentary Pa/Th response to forced global particle flux decrease. Sedimentary Pa/Th anomalies (sensitivities studies − PI control run). The areas in white did not display significant changes compared to the natural variability (i.e. anomalies <4σ − see methods). The changes in all/2 reflect the combination of changes in POC/2, opal/2 and CaCO3/2, even if not clearly apparent on the figure as changes less than 4σ are not shown.

low impact of $CaCO_3$ on Pa/Th is related to the low affinity of Pa for this particle type (Table 1) and to low $CaCO_3$ concentrations (Fig. 1).

To summarize, we have seen that in our simulations POC is the dominant particle that transfers Pa to the sediments in the Atlantic Ocean, while opal is the main scavenger in regions where NEMO-PISCES simulated high opal concentrations, i.e. in the Southern Ocean and along the North American continental margins (between 30°N and 50°N and around 40°S). $CaCO_3$ has the smallest impact on sedimentary Pa/Th, consistent with the low affinity of Pa for $CaCO_3$ (Table 1) and lower particle concentrations. Despite some spatial variability, reducing the particle concentration tends to increase Pa accumulation in the sediments of the open ocean and subtropical gyres. Our study suggests that the sedimentary Pa/Th response to a 50% particle concentration decrease i) exceeds the natural Pa/Th variability under PI conditions, leading to mean Pa/Th changes of 0.01, and ii) strongly depends on the particle fields and their geographical distribution.

3.3. Impact of a change in phytoplankton type

In this section we analyze the results of a simulation where we mimic a global change in plankton community at constant POC production by halving the opal flux and doubling the $CaCO_3$ flux (see methods). This is informative on the respective role of the two particle types in driving sedimentary Pa/Th changes in the different regions of the Atlantic basin. In the opal_2_CaCO3x2 simulation, sedimentary Pa/Th strongly decreases by 0.02 in the Southern Ocean around 40°S and in particular in the southeastern Atlantic basin (Fig. 5). Pa/Th also decreases along the American margin (between 30°N and 50°N) by 0.015 and to a lesser extent between 20°S and the equator where the decrease is less than 0.01. Elsewhere the sedimentary Pa/Th increases, in particular in the North Atlantic between 0 and 40°N by about 0.01 and off the African coast by up to 0.015 (Fig. 5). Overall, the sedimentary Pa/Th pattern in the opal_2_CaCO3x2 simulation is similar to the pattern obtained in the opal_2 simulation in the North Atlantic and in the Southern Ocean (south of 40°S) and to the CaCO3x2 simulation in the equatorial south Atlantic and along the African coast (between 40°S and 20°N) (Fig. 5). The sedimentary Pa/Th is therefore mostly affected by changes in opal flux in the North Atlantic and in the Southern Ocean (south of 40°S), while it is predominantly affected by changes in $CaCO_3$ flux in the equatorial south Atlantic and off the African coast (between 40°S and 20°N).

4. Discussion

4.1. Potential changes in particle fluxes across climatic transitions

There is compelling evidence of marked productivity changes across climatic transitions (e.g. Jaccard et al., 2013; Kohfeld et al., 2005) associated with variations of biogenic particles (POC, CaCO3 and opal) production (e.g. Yamamoto et al., 2019) and burial (Cartapanis et al., 2018, 2016). However, quantitative reconstructions of changes in particle fluxes across climatic transitions are currently limited by 1) the lack of Atlantic-wide compilations of proxy-based reconstructions, 2) discrepancies between model outputs when different models are run under similar boundary conditions (e.g. (Kageyama et al., 2013a, 2013b)). Despite these limitations, both proxy data and climate models consistently suggest a decrease in productivity in the North Atlantic while the productivity might have increased slightly in the Southern Ocean and in equatorial regions during Heinrich stadials (e.g. (Brown and Galbraith, 2016; Mariotti et al., 2012 and references therein, Martínez-García et al., 2014; Straub et al., 2013)). Modelling studies (Brown and Galbraith, 2016; Mariotti et al., 2012) estimate that the export productivity could have decreased by about 50% in the North Atlantic during an Heinrich stadial. In this study we have explored the impact of similar large-scale variations in export productivity by doubling or halving the particle fluxes in our simulations.

4.2. Sensitivity of sedimentary Pa/Th to particles versus circulation changes

A recent compilation of Pa/Th records covering the last deglaciation in the Atlantic basin (Ng et al., 2018) shows that most of the northwest Atlantic cores display a marked ~0.03 Pa/Th units increase between the LGM and Heinrich stadial 1. Such Pa/Th variations have also been observed for other millennial scale events (e.g. Böhm et al., 2015; Burckel et al., 2016, 2015; Waelbroeck et al., 2018). Our sensitivity study shows that a 50% change in biogenic particle flux intensity can lead to a variation in Pa/Th of ~0.01, which corresponds to about 30% of the observed Pa/Th increase across Heinrich stadial 1.

By comparison, in iLOVECLIM, a ~250 years AMOC shutdown under PI boundary conditions causes a consistent Pa/Th increase of about 0.03 in the northwest Atlantic (40°N - 60°N) between 2000 and 3000 m water depth (Missiaen et al., 2020). This is consistent

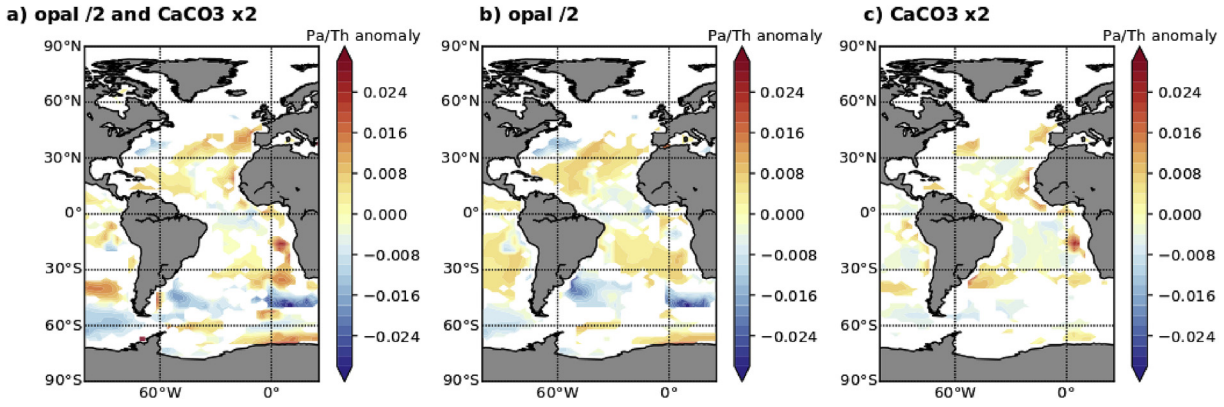

Fig. 5. Effect of a change in plankton community on the sedimentary Pa/Th. As on Fig. 4, sedimentary Pa/Th anomalies are represented (sensitivities studies − PI control run). The areas in white did not display significant changes compared to the natural variability (i.e. anomalies $<4\sigma$ − see methods). Opal concentrations are halved, while $CaCO_3$ concentrations are doubled and POC concentrations are maintained constant.

with the simulated Pa/Th variations obtained in other model studies (Gu and Liu, 2017; Rempfer et al., 2017; Siddall et al., 2007). However, at the Bermuda Rise location (~34°N, 58°W, > 4300 m), where the first Pa/Th time series has been obtained (McManus et al., 2004), the Pa/Th increases by ~ 0.01 in iLOVECLIM, which is less than the observed Pa/Th variation recorded at this location across Heinrich stadial 1. However, this particular hosing experiment is not an analogue to a Heinrich event, because the simulation was integrated under preindustrial (not glacial) boundary conditions, the freshwater was only added to the Nordic Seas, and the AMOC was shut down for a relatively short duration (~300 years), which is shorter than what is observed during Heinrich stadial 1 (>1000 years) (see (Missiaen et al., 2020)). In addition, the Bermuda Rise lies in the transition zone between the coastal region with high particle fluxes and the open ocean in iLOVECLIM (see Fig. 1), complicating direct model-data comparison at this specific location. The particle-induced Pa/Th variations simulated in this study are therefore significant and of the same order of magnitude (30–100%) than the simulated changes obtained during an AMOC shutdown.

It is important to note that the amplitude of Pa/Th variations due to a circulation slowdown was tested in iLOVECLIM with an AMOC strength of ~17 Sv, but a rather shallow NADW (~2500 m) compared to observations (Lozier et al., 2019). As Pa concentrations typically increase with depth (Henderson and Anderson, 2003), the depth of NADW may impact the southward transport of Pa in the model. Any change in the boundary conditions, such as for example the reference climate state (e.g. LGM), and subsequent changes in the Atlantic water masses configuration, will also likely impact the sensitivity of the sedimentary Pa/Th to changes in particle fluxes. In line with previous studies, we find that in regions with sluggish circulation (typically outside of the deep western boundary current), the impact of particle fluxes variations (e.g. in coastal areas) could have an even larger impact on sedimentary Pa/Th. Indeed, in these regions, the particle-induced Pa transport is a dominant process that can overcome the circulation-induced Pa transport (Gu and Liu, 2017).

To date, attempts to achieve quantitative reconstructions of the AMOC strength variations rely on fitting a Pa/Th enabled model to observed Pa/Th variations from Atlantic sediment cores. However, the skill of a Pa/Th model to predict the sedimentary Pa/Th response to abrupt circulation changes depends on its ability to capture the "right" balance between Pa and Th transport by advection and Pa and Th transport induced by particle flux gradients (i.e. the scavenging regime). Future work is therefore needed to further evaluate the sensitivity of iLOVECLIM and other Pa/Th enabled models to circulation and particle fluxes changes.

4.3. Evaluation of the Pa and Th transport in iLOVECLIM

One way to further assess how Pa and Th are transported in a model consists in analyzing the normalized Pa and Th fluxes to the sediments i.e. the ratio between the fluxes to the sediments (particulate Pa and Th) and the local water column production (Fig. 1-see section 3.1). Model studies first estimated that up to 30% of the Th is transported and deposited away from the water column where it has been produced (Henderson et al., 1999). A recent analysis of the new GEOTRACES water column data revised this estimate to ~40% (Hayes et al., 2015a), which was confirmed by the recent review and compilation of ^{230}Th sedimentary data of (Costa et al., 2020). In other words, assuming that Th settles fast enough to stay in the Atlantic basin, the ratio between the Th flux to the sediments and the local water column production should range between ~0.6 and 1.4. In iLOVECLIM, the range of normalized Th flux is slightly wider (from ~0.4 to 1.6) in the PI control simulation, meaning that Th transport (mostly by particle gradients) is likely slightly overestimated. The normalized Th flux from different models embedding Pa and Th has been shown to often resemble the biological productivity pattern as observed here in iLOVECLIM. However, while iLOVECLIM produces normalized Th fluxes relatively close to 1, a larger range in normalized Th fluxes has been evidenced in other models (Costa et al., 2020). Future work is needed to evaluate how the scavenging regimes are represented across different Earth system models embedding Pa and Th isotopes, as well as how the different model structures and parametrization choices influence the sedimentary Pa/Th.

4.4. Impact of far field changes in particle fluxes on Pa/Th records

Our sensitivity experiments highlight that the sedimentary Pa/Th response has a geographical pattern that is tightly related to the geographical distribution of the particles and the spatial distribution of high scavenging intensity areas. In regions where Pa and Th are dominantly scavenged to the sediments by a certain particle type, a greater flux of this particle type increases the Pa/Th ratio (as expected). Where this particle type is not the dominant scavenger, the opposite effect happens. When reducing the scavenging intensity in a neighboring region, the Pa/Th is found to increase outside the main scavenging areas as more Pa can escape from the high scavenging areas and settle down in the open ocean sediments. In particular, our study suggests that an opal production decrease off the North American coast (between 30°N and 50°N - corresponding in our model to a high opal flux area) may induce a significant Pa/Th increase in a large part of the North Atlantic basin, where opal production is low and where most of the available Pa/Th records are located (Figs. 1–4). A decrease in the particle fluxes results in an increase in the residence time of Pa and Th in the water column. The fact that in our model more Pa settles in the North Atlantic when we decrease the particle fluxes globally is due to reduced Pa scavenging along the American coast (between 30°N and 50°N). The presence of opal in the North Atlantic under modern conditions is corroborated by modern observations (van Hulten et al., 2018). Additionally, there is evidence in the sediments for a North Atlantic opal belt (Lippold et al., 2012a; Seiter et al., 2004) south of Iceland while in the model the North Atlantic opal belt is located closer to the North American coast.

The fact that Pa can be burried in the North Atlantic sediments when the general scavenging intensity decreases also suggests that relatively low amounts of Pa are transported towards the Southern Ocean in the central North Atlantic in our model. This may be related to the relatively shallow NADW (lower boundary ~2500 m) compared to observations, given that the highest concentrations of Pa are generally found at greater depths and/or in regions with sluggish circulation outside of the deep western boundary current. Further work is needed to investigate the mechanisms of Pa transport in other Pa/Th enabled models.

From the data side (Gherardi et al., 2009), reported an inverse relationship between the reconstructed diatom flux (hence opal flux) and the sedimentary Pa/Th in core MD95-2027 located in the northwest Atlantic, which is consistent with our sensitivity experiment results. The potential of changes in biogenic particle fluxes and composition to increase the sedimentary Pa/Th ratio has been largely acknowledged in the literature, with a particular concern for opal, for which Pa has a very strong affinity (Chase et al., 2002). The impact of potential changes in opal flux on sedimentary Pa/Th has been assessed by different means. Some studies argued that the opal content of the core(s) remained low (generally < 5 wt %) throughout the studies time interval (Böhm et al., 2015; Lippold et al., 2016, 2012a). Other studies highlighted that there was no

correlation between the Pa/Th and the ^{230}Th-normalized opal flux and/or ^{230}Th-normalized diatom valves flux records in the sediment core (e.g. (Gherardi et al., 2009; Mulitza et al., 2017; Nave et al., 2007). Our study confirms that in addition to the site-specific particle flux variations, the basin-wide and/or regional particle fluxes may have also impacted the paleo Pa/Th records. Revisiting the available Pa/Th records would thus require an extensive basin-wide evaluation of the particle flux evolution and/or evaluation of the Pa budget in the Atlantic basin (Hayes et al., 2014) throughout the deglaciation.

Finally, our sensitivity experiments with iLOVECLIM show that uniform changes in particle concentrations affect the Pa/Th ratio distribution differently depending on the particle type, and our model suggests that changes in POC may influence the sedimentary Pa/Th ratio more than opal. From the observational side, changes in POC concentrations have not been monitored along with the Pa/Th time series, mostly because sedimentary POC content is prone to be modified by post-deposition remineralization processes. In our simulations, the high sensitivity of the sedimentary Pa/Th to POC could potentially originate from two distinct model features: 1) an over-representation of POC concentrations in the particle forcing fields and/or 2) the choice of scavenging coefficients that give Pa and Th high affinity for POC (see Table 1). The prescribed particle concentration fields used in this study have been evaluated against modern data in (van Hulten et al., 2018) and the POC concentrations appear to be slightly overestimated in the upper 200 m of the water column, but generally underestimated in the oligotrophic regions such as the subtropical gyres. Additional observations of particulate concentrations in the water column are required to better assess the quality of the POC representation in NEMO-PISCES. The coefficients are tunable parameters that have been determined using an objective exploration of the parameter space (Missiaen et al., 2020) and set to obtain the best fit between sedimentary Pa/Th, dissolved and particulate water column Pa and Th. The scavenging coefficients that are used in iLOVECLIM are significantly higher than observations (Hayes et al., 2015b). However, decreasing the scavenging coefficients towards the values determined by (Hayes et al., 2015b) dramatically decreases model data agreements in the water column, suggesting that the model needs high scavenging coefficients to remove enough Pa and Th from the water column. This is consistent with the conclusions from previous studies (e.g. Dutay et al., 2009), which found that scavenging coefficients are implicitly inversely scaled to the particle fluxes in order to simulate a scavenging intensity compatible with observations. Further model intercomparison work is needed to investigate whether the high sensitivity of sedimentary Pa/Th to POC is a robust feature across different representations of Pa and Th scavenging in different models.

5. Conclusions and perspectives

We have performed a set of idealized simulations using the Earth System model of intermediate complexity iLOVECLIM in order to study the large-scale relation between sedimentary Pa/Th and biogenic particle fluxes in the water column. Our results show that changes in particle fluxes due to changes in biogenic export productivity can significantly impact sedimentary Pa/Th. Our simulations suggest that the Pa/Th response is sensitive to the geographical distribution of particles and intense scavenging areas; for example, a decrease in the opal fluxes off the North American coast (between 30°N and 50°N), where in our reference preindustrial simulations the opal fluxes are relatively high, induces a sedimentary Pa/Th increase in most of the North Atlantic basin, outside of the high opal scavenging area. Far field changes in opal production might therefore impact the sedimentary Pa/Th, even in low opal production areas. Our simulations show that depending on the particle type, uniform changes in particle fluxes affect the spatial distribution of the Pa/Th ratio differently (Figs. 4–5). They also highlight a potential dominant role of POC in driving Pa/Th changes, followed by opal. Further work is necessary to assess if this result is a robust feature across different models able to simulate the evolution of Pa and Th in the ocean. Halving the particle fluxes, as might have happened during Heinrich stadial 1, leads to a Pa/Th increase of about 0.01, corresponding to ~30% of the observed Pa/Th increase in the North Atlantic across Heinrich stadial 1. This corresponds to at least one third and up to the full amplitude of sedimentary Pa/Th changes simulated during an AMOC shutdown by the same model, suggesting that in this model framework, the sedimentary Pa/Th has a similar sensitivity to circulation and particle flux changes. The ability of a model to capture the amplitude of Pa/Th changes associated with abrupt climate change is related to its ability to capture the right balance between the circulation-related and the particle-related transport, which ultimately depends on the representation of the deep-water circulation, particle fluxes and the scavenging parameters. Further progress in assessing the impact of particle-induced sedimentary Pa/Th changes therefore requires i) a thorough evaluation of past geographical particles patterns, and ii) a skillful representation of the scavenging regime and water mass pathways, which would require an in-depth Pa/Th model intercomparison.

Author contributions

LM, LCM and KJM designed the research. LM, DMR, NB, JCD AQ and FL developed the iLOVECLIM model. LM performed the simulations and data curation. JCD and SP contributed to expert knowledge on Pa/Th. LM wrote the manuscript with the inputs form all the co-authors. CW, KJM and LCM obtained the funding.

Lise Missiaen: Conceptualization, Investigation, Methodology, Validation, Visualization, Writing- original draft. **Laurie C. Menviel**: Supervision, Writing-review and editing, Funding acquisition. **Katrin J. Meissner**: Supervision, Writing-review and editing, Funding acquisition. **Didier M. Roche**: Resources, Methodology, Software, Writing-review and editing. **Nathaelle Bouttes**: Methodology, Software, Writing-review and editing. **Jean-Claude Dutay**: Methodology, Writing-review and editing. **Aurélien Quiquet**: Methodology, Software, Writing-review and editing. **Fanny Lhardy**: Methodology, Software, Writing-review and editing. **Sylvain Pichat**: Writing-review and editing. **Claire Waelbroeck**: Writing-review and editing, Funding acquisition

Code and data availability

The iLOVECLIM source code is based on the LOVECLIM model version 1.2 whose code is accessible at http://www.elic.ucl.ac.be/modx/elic/index.php?id=289. The developments on the iLOVECLIM source code are hosted at https://forge.ipsl.jussieu.fr/ludus but are not publicly available due to copyright restrictions. Access can be granted on demand by request to D. M. Roche (didier.roche@lsce.ipsl.fr).

The model output related to this article will be submitted to https://pangaea.de/.

Declaration of competing interest

The authors declare that they have no conflict of interests.

Acknowledgements

This is a contribution to ERC project ACCLIMATE; the research leading to these results has received funding from the European Research Council under the European Union's Seventh Framework Programme (FP7/2007–2013)/ERC grant agreement 339108. KJM, LCM and LM acknowledge funding from the Australian Research Council grant DP180100048 awarded to KJM and LCM and grant FT180100606 awarded to LCM. We thank S. Moreira and for his help with Python.

Appendix A. Supplementary data

Supplementary data to this article can be found online at https://doi.org/10.1016/j.quascirev.2020.106394.

References

Anderson, R.F., Bacon, M.P., Brewer, P.G., 1983. Removal of 230 Th and 231 Pa at ocean margins. Earth Planet Sci. Lett. 66, 73–90.

Anderson, R.F., Cheng, H., Edwards, R.L., Fleisher, M.Q., Hayes, C.T., Huang, K.-F., Kadko, D., Lam, P.J., Landing, W.M., Lao, Y., 2016. How well can we quantify dust deposition to the ocean? Phil. Trans. Math. Phys. Eng. Sci. 374, 20150285.

Bacon, M.P., Anderson, R.F., 1982. Distribution of thorium isotopes between dissolved and particulate forms in the deep sea. J. Geophys. Res.: Oceans 87, 2045–2056. https://doi.org/10.1029/JC087iC03p02045.

Böhm, E., Lippold, J., Gutjahr, M., Frank, M., Blaser, P., Antz, B., Fohlmeister, J., Frank, N., Andersen, M.B., Deininger, M., 2015. Strong and deep Atlantic meridional overturning circulation during the last glacial cycle. Nature 517, 73–76.

Bopp, L., Aumont, O., Cadule, P., Alvain, S., Gehlen, M., 2005. Response of diatoms distribution to global warming and potential implications: a global model study. Geophys. Res. Lett. 32 https://doi.org/10.1029/2005GL023653.

Brown, N., Galbraith, E.D., 2016. Hosed vs. unhosed: interruptions of the Atlantic Meridional Overturning Circulation in a global coupled model, with and without freshwater forcing. Clim. Past 12, 1663–1679. https://doi.org/10.5194/cp-12-1663-2016.

Brzezinski, M.A., Pride, C.J., Franck, V.M., Sigman, D.M., Sarmiento, J.L., Matsumoto, K., Gruber, N., Rau, G.H., Coale, K.H., 2002. A switch from Si (OH) 4 to NO3− depletion in the glacial Southern Ocean. Geophys. Res. Lett. 29, 5-1-5–4.

Burckel, P., Waelbroeck, C., Gherardi, J.M., Pichat, S., Arz, H., Lippold, J., Dokken, T., Thil, F., 2015. Atlantic Ocean circulation changes preceded millennial tropical South America rainfall events during the last glacial. Geophys. Res. Lett. 42, 411–418.

Burckel, P., Waelbroeck, C., Luo, Y., Roche, D.M., Pichat, S., Jaccard, S.L., Gherardi, J., Govin, A., Lippold, J., Thil, F., 2016. Changes in the geometry and strength of the Atlantic meridional overturning circulation during the last glacial (20-50ka). Clim. Past 12, 2061.

Cartapanis, O., Bianchi, D., Jaccard, S.L., Galbraith, E.D., 2016. Global pulses of organic carbon burial in deep-sea sediments during glacial maxima. Nat. Commun. 7, 10796.

Cartapanis, O., Galbraith, E.D., Bianchi, D., Jaccard, S., 2018. Carbon burial in deep-sea sediment and implications for oceanic inventories of carbon and alkalinity over the last glacial cycle. Clim. Past 14, 1819–1850.

Chase, Z., Anderson, R.F., Fleisher, M.Q., Kubik, P.W., 2003. Scavenging of 230Th, 231Pa and 10Be in the Southern Ocean (SW Pacific sector): the importance of particle flux, particle composition and advection. Deep Sea Res. Part II Top. Stud. Oceanogr. 50, 739–768. https://doi.org/10.1016/S0967-0645(02)00593-3.

Chase, Z., Anderson, R.F., Fleisher, M.Q., Kubik, P.W., 2002. The influence of particle composition and particle flux on scavenging of Th, Pa and Be in the ocean. Earth Planet Sci. Lett. 204, 215–229. https://doi.org/10.1016/S0012-821X(02)00984-6.

Conte, M.H., Ralph, N., Ross, E.H., 2001. Seasonal and interannual variability in deep ocean particle fluxes at the Oceanic Flux Program (OFP)/Bermuda Atlantic Time Series (BATS) site in the western Sargasso Sea near Bermuda. Deep Sea Res. Part II Top. Stud. Oceanogr. 48, 1471–1505. https://doi.org/10.1016/S0967-0645(00)00150-8.

Costa, K.M., Hayes, C.T., Anderson, R.F., Pavia, F.J., Bausch, A., Deng, F., Dutay, J.-C., Geibert, W., Heinze, C., Henderson, G., Hillaire-Marcel, C., Hoffmann, S., Jaccard, S.L., Jacobel, A.W., Kienast, S.S., Kipp, L., Lerner, P., Lippold, J., Lund, D., Marcantonio, F., McGee, D., McManus, J.F., Mekik, F., Middleton, J.L., Missiaen, L., Not, C., Pichat, S., Robinson, L.F., Rowland, G.H., Roy-Barman, M., Tagliabue, A., Torfstein, A., Winckler, G., Zhou, Y., 2020. 230Th normalization: new insights on an essential tool for quantifying sedimentary fluxes in the modern and quaternary ocean. Paleoceanogr. Paleoclimatol. 35, e2019PA003820 https://doi.org/10.1029/2019PA003820.

Deng, F., Henderson, G.M., Castrillejo, M., Perez, F.F., Steinfeldt, R., 2018. Evolution of 231Pa and 230Th in overflow waters of the north Atlantic. Biogeosciences 15, 7299–7313. https://doi.org/10.5194/bg-15-7299-2018.

Deng, F., Thomas, A.L., Rijkenberg, M.J.A., Henderson, G.M., 2014. Controls on seawater 231Pa, 230Th and 232Th concentrations along the flow paths of deep waters in the Southwest Atlantic. Earth Planet Sci. Lett. 390, 93–102. https://doi.org/10.1016/j.epsl.2013.12.038.

Dunne, J.P., Sarmiento, J.L., Gnanadesikan, A., 2007. A synthesis of global particle export from the surface ocean and cycling through the ocean interior and on the seafloor. Global Biogeochem. Cycles 21. https://doi.org/10.1029/2006GB002907.

Dutay, J.-C., Lacan, F., Roy-Barman, M., Bopp, L., 2009. Influence of particle size and type on 231Pa and 230Th simulation with a global coupled biogeochemical-ocean general circulation model: a first approach. G-cubed 10.

Farrell, J.W., Prell, W.L., 1989. Climatic change and CaCO3 preservation: an 800,000 year bathymetric reconstruction from the central equatorial Pacific Ocean. Paleoceanography 4, 447–466.

François, R., 2007. Paleoflux and Paleocirculation from Sediment 230Th and 231Pa/230Th. Proxies in Late Cenozoic Paleoceanography. Elsevier, pp. 681–716.

Gdaniec, S., Roy-Barman, M., Foliot, L., Thil, F., Dapoigny, A., Burckel, P., Garcia-Orellana, J., Masqué, P., Mörth, C.-M., Andersson, P.S., 2018. Thorium and protactinium isotopes as tracers of marine particle fluxes and deep water circulation in the Mediterranean Sea. Mar. Chem. 199, 12–23.

Gherardi, J.M., Labeyrie, L., Nave, S., Francois, R., McManus, J.F., Cortijo, E., 2009. Glacial-interglacial circulation changes inferred from 231Pa/230Th sedimentary record in the North Atlantic region. Paleoceanography 24. https://doi.org/10.1029/2008PA001696 n/a-n/a.

Goosse, H., Brovkin, V., Fichefet, T., Haarsma, R., Huybrechts, P., Jongma, J., Mouchet, A., Selten, F., Barriat, P.-Y., Campin, J.-M., 2010. Description of the Earth system model of intermediate complexity LOVECLIM version 1.2. Geosci. Model Dev. (GMD) 3, 603–633.

Gu, S., Liu, Z., 2017. 231 Pa and 230 Th in the Ocean model of the community Earth system model (CESM1. 3). Geosci. Model Dev. (GMD) 10.

Hayes, C.T., Anderson, R.F., Fleisher, M.Q., Huang, K.-F., Robinson, L.F., Lu, Y., Cheng, H., Edwards, R.L., Moran, S.B., 2015a. 230Th and 231Pa on GEOTRACES GA03, the U.S. GEOTRACES North Atlantic transect, and implications for modern and paleoceanographic chemical fluxes. Deep Sea Res. Part II Top. Stud. Oceanogr. 116, 29–41. https://doi.org/10.1016/j.dsr2.2014.07.007.

Hayes, C.T., Anderson, R.F., Fleisher, M.Q., Serno, S., Winckler, G., Gersonde, R., 2014. Biogeography in 231Pa/230Th ratios and a balanced 231Pa budget for the Pacific Ocean. Earth Planet Sci. Lett. 391, 307–318. https://doi.org/10.1016/j.epsl.2014.02.001.

Hayes, C.T., Anderson, R.F., Fleisher, M.Q., Vivancos, S.M., Lam, P.J., Ohnemus, D.C., Huang, K.-F., Robinson, L.F., Lu, Y., Cheng, H., Edwards, R.L., Moran, S.B., 2015b. Intensity of Th and Pa scavenging partitioned by particle chemistry in the North Atlantic Ocean. Mar. Chem. 170, 49–60. https://doi.org/10.1016/j.marchem.2015.01.006.

Hemming, S.R., 2004. Heinrich events: massive late Pleistocene detritus layers of the North Atlantic and their global climate imprint. Rev. Geophys. 42.

Henderson, G.M., Anderson, R.F., 2003. The U-series toolbox for paleoceanography. Rev. Mineral. Geochem. 52, 493–531. https://doi.org/10.2113/0520493.

Henderson, G.M., Heinze, C., Anderson, R.F., Winguth, A.M.E., 1999. Global distribution of the 230Th flux to ocean sediments constrained by GCM modelling. Deep Sea Res. Oceanogr. Res. Pap. 46, 1861–1893. https://doi.org/10.1016/S0967-0637(99)00030-8.

Jaccard, S.L., Hayes, C.T., Martínez-García, A., Hodell, D.A., Anderson, R.F., Sigman, D.M., Haug, G.H., 2013. Two modes of change in Southern Ocean productivity over the past million years. Science 339, 1419. https://doi.org/10.1126/science.1227545.

Kageyama, M., Braconnot, P., Bopp, L., Caubel, A., Foujols, M.-A., Guilyardi, E., Khodri, M., Lloyd, J., Lombard, F., Mariotti, V., 2013a. Mid-holocene and last glacial maximum climate simulations with the IPSL model—Part I: comparing IPSL_CM5A to IPSL_CM4. Clim. Dynam. 40, 2447–2468.

Kageyama, M., Braconnot, P., Bopp, L., Mariotti, V., Roy, T., Woillez, M.-N., Caubel, A., Foujols, M.-A., Guilyardi, E., Khodri, M., 2013b. Mid-Holocene and last glacial maximum climate simulations with the IPSL model: part II: model-data comparisons. Clim. Dynam. 40, 2469–2495.

Kienast, S.S., Winckler, G., Lippold, J., Albani, S., Mahowald, N.M., 2016. Tracing dust input to the global ocean using thorium isotopes in marine sediments: ThoroMap. Global Biogeochem. Cycles 30, 1526–1541. https://doi.org/10.1002/2016GB005408.

Kohfeld, K.E., Le Quéré, C., Harrison, S.P., Anderson, R.F., 2005. Role of marine biology in glacial-interglacial CO2 cycles. Science 308, 74–78.

Krishnaswami, S., Lal, D., Somayajulu, B.L.K., Weiss, R.F., Craig, H., 1976. Large-volume in-situ filtration of deep Pacific waters: mineralogical and radioisotope studies. Earth Planet Sci. Lett. 32, 420–429.

Le, J., Shackleton, N.J., 1992. Carbonate dissolution fluctuations in the western equatorial pacific during the late quaternary. Paleoceanography 7, 21–42. https://doi.org/10.1029/91PA02854.

Lippold, J., Gherardi, J.-M., Luo, Y., 2011. Testing the 231Pa/230Th paleocirculation proxy: a data versus 2D model comparison. Geophys. Res. Lett. 38 https://doi.org/10.1029/2011GL049282.

Lippold, J., Grützner, J., Winter, D., Lahaye, Y., Mangini, A., Christl, M., 2009. Does sedimentary 231Pa/230Th from the Bermuda Rise monitor past Atlantic meridional overturning circulation? Geophys. Res. Lett. 36.

Lippold, J., Gutjahr, M., Blaser, P., Christner, E., de Carvalho Ferreira, M.L., Mulitza, S., Christl, M., Wombacher, F., Böhm, E., Antz, B., Cartapanis, O., Vogel, H., Jaccard, S.L., 2016. Deep water provenance and dynamics of the (de)glacial

Atlantic meridional overturning circulation. Earth Planet Sci. Lett. 445, 68–78. https://doi.org/10.1016/j.epsl.2016.04.013.
Lippold, J., Luo, Y., Francois, R., Allen, S.E., Gherardi, J., Pichat, S., Hickey, B., Schulz, H., 2012a. Strength and geometry of the glacial Atlantic meridional overturning circulation. Nat. Geosci. 5, 813.
Lippold, J., Mulitza, S., Mollenhauer, G., Weyer, S., Heslop, D., Christl, M., 2012b. Boundary scavenging at the East Atlantic margin does not negate use of 231Pa/230Th to trace Atlantic overturning. Earth Planet Sci. Lett. 333–334, 317–331. https://doi.org/10.1016/j.epsl.2012.04.005.
Lozier, M.S., Li, F., Bacon, S., Bahr, F., Bower, A.S., Cunningham, S.A., de Jong, M.F., de Steur, L., deYoung, B., Fischer, J., Gary, S.F., Greenan, B.J.W., Holliday, N.P., Houk, A., Houpert, L., Inall, M.E., Johns, W.E., Johnson, H.L., Johnson, C., Karstensen, J., Koman, G., Le Bras, I.A., Lin, X., Mackay, N., Marshall, D.P., Mercier, H., Oltmanns, M., Pickart, R.S., Ramsey, A.L., Rayner, D., Straneo, F., Thierry, V., Torres, D.J., Williams, R.G., Wilson, C., Yang, J., Yashayaev, I., Zhao, J., 2019. A sea change in our view of overturning in the subpolar North Atlantic. Science 363, 516–521.
Luo, S., Ku, T.-L., 2004. On the importance of opal, carbonate, and lithogenic clays in scavenging and fractionating 230Th, 231Pa and 10Be in the ocean. Earth Planet Sci. Lett. 220, 201–211.
Luo, S., Ku, T.-L., 1999. Oceanic 231Pa/230Th ratio influenced by particle composition and remineralization. Earth Planet Sci. Lett. 167, 183–195.
Luo, Y., Francois, R., Allen, S.E., 2010. Sediment 231Pa/230Th as a recorder of the rate of the Atlantic meridional overturning circulation: insights from a 2-D model. Ocean Sci. Discuss. 6, 2755–2829.
Lynch-Stieglitz, J., 2017. The Atlantic meridional overturning circulation and abrupt climate change. Ann. Rev. Mar. Sci. 9, 83–104. https://doi.org/10.1146/annurev-marine-010816-060415.
Marchal, O., François, R., Stocker, T.F., Joos, F., 2000. Ocean thermohaline circulation and sedimentary 231Pa/230Th ratio. Paleoceanography 15, 625–641.
Marinov, I., Doney, S.C., Lima, I.D., 2010. Response of ocean phytoplankton community structure to climate change over the 21st century: partitioning the effects of nutrients, temperature and light. Biogeosciences 7, 3941–3959. https://doi.org/10.5194/bg-7-3941-2010.
Mariotti, V., Bopp, L., Tagliabue, A., Kageyama, M., Swingedouw, D., 2012. Marine productivity response to Heinrich events: a model-data comparison. Clim. Past 8, 1581–1598.
Martínez-García, A., Sigman, D.M., Ren, H., Anderson, R.F., Straub, M., Hodell, D.A., Jaccard, S.L., Eglinton, T.I., Haug, G.H., 2014. Iron fertilization of the subantarctic ocean during the last ice age. Science 343, 1347. https://doi.org/10.1126/science.1246848.
Matsumoto, K., Sarmiento, J.L., Brzezinski, M.A., 2002. Silicic acid leakage from the Southern Ocean: a possible explanation for glacial atmospheric pCO2. Global Biogeochem. Cycles 16, 5-1-5–23.
McManus, J.F., Francois, R., Gherardi, J.-M., Keigwin, L.D., Brown-Leger, S., 2004. Collapse and rapid resumption of Atlantic meridional circulation linked to deglacial climate changes. Nature 428, 834–837.
Menviel, L., Timmermann, A., Mouchet, A., Timm, O., 2008. Meridional reorganizations of marine and terrestrial productivity during Heinrich events. Paleoceanography 23. https://doi.org/10.1029/2007PA001445.
Missiaen, L., Bouttes, N., Roche, D.M., Dutay, J.-C., Quiquet, A., Waelbroeck, C., Pichat, S., Peterschmitt, J.-Y., 2020. Carbon isotopes and Pa/Th response to forced circulation changes: a model perspective. Clim. Past 16, 867–883. https://doi.org/10.5194/cp-16-867-2020.
Missiaen, L., Pichat, S., Waelbroeck, C., Douville, E., Bordier, L., Dapoigny, A., Thil, F., Foliot, L., Wacker, L., 2018. Downcore variations of sedimentary detrital (238U/232Th) ratio: implications on the use of 230Thxs and 231Paxs to reconstruct sediment flux and ocean circulation. G-cubed. https://doi.org/10.1029/2017GC007410.
Mulitza, S., Chiessi, C.M., Schefuß, E., Lippold, J., Wichmann, D., Antz, B., Mackensen, A., Paul, A., Prange, M., Rehfeld, K., 2017. Synchronous and proportional deglacial changes in Atlantic Meridional Overturning and northeast Brazilian precipitation. Paleoceanography.
Nave, S., Labeyrie, L., Gherardi, J., Caillon, N., Cortijo, E., Kissel, C., Abrantes, F., 2007. Primary productivity response to Heinrich events in the north Atlantic Ocean and Norwegian sea. Paleoceanogr. Paleoclimatol. 22.
Ng, H.C., Robinson, L.F., McManus, J.F., Mohamed, K.J., Jacobel, A.W., Ivanovic, R.F., Gregoire, L.J., Chen, T., 2018. Coherent deglacial changes in western Atlantic Ocean circulation. Nat. Commun. 9.
Nozaki, Y., Horibe, Y., Tsubota, H., 1981. The water column distributions of thorium isotopes in the western North Pacific. Earth Planet Sci. Lett. 54, 203–216.
Rahmstorf, S., 2002. Ocean circulation and climate during the past 120,000 years. Nature 419, 207. https://doi.org/10.1038/nature01090.
Rempfer, J., Stocker, T.F., Joos, F., Lippold, J., Jaccard, S.L., 2017. New insights into cycling of 231Pa and 230Th in the Atlantic Ocean. Earth Planet Sci. Lett. 468, 27–37. https://doi.org/10.1016/j.epsl.2017.03.027.
Richaud, M., Loubere, P., Pichat, S., Francois, R., 2007. Changes in opal flux and the rain ratio during the last 50,000 years in the equatorial Pacific. Deep Sea Res. Part II Top. Stud. Oceanogr. 54, 762–771.
Roy-Barman, M., 2009. Modelling the effect of boundary scavenging on Thorium and Protactinium profiles in the ocean. Biogeosciences 6, 3091–3107. https://doi.org/10.5194/bg-6-3091-2009.
Schmittner, A., 2005. Decline of the marine ecosystem caused by a reduction in the Atlantic overturning circulation. Nature 434, 628.
Seiter, K., Hensen, C., Schröter, J., Zabel, M., 2004. Organic carbon content in surface sediments—defining regional provinces. Deep Sea Res. Oceanogr. Res. Pap. 51, 2001–2026. https://doi.org/10.1016/j.dsr.2004.06.014.
Siddall, M., Henderson, G.M., Edwards, N.R., Frank, M., Müller, S.A., Stocker, T.F., Joos, F., 2005. 231Pa/230Th fractionation by ocean transport, biogenic particle flux and particle type. Earth Planet Sci. Lett. 237, 135–155. https://doi.org/10.1016/j.epsl.2005.05.031.
Siddall, M., Stocker, T.F., Henderson, G.M., Joos, F., Frank, M., Edwards, N.R., Ritz, S.P., Müller, S.A., 2007. Modeling the relationship between 231Pa/230Th distribution in North Atlantic sediment and Atlantic meridional overturning circulation. Paleoceanography 22. https://doi.org/10.1029/2006PA001358.
Stephens, M.P., Kadko, D.C., 1997. Glacial-Holocene calcium carbonate dissolution at the central equatorial Pacific seafloor. Paleoceanography 12, 797–804.
Straub, M., Tremblay, M.M., Sigman, D.M., Studer, A.S., Ren, H., Toggweiler, J.R., Haug, G.H., 2013. Nutrient conditions in the subpolar North Atlantic during the last glacial period reconstructed from foraminifera-bound nitrogen isotopes. Paleoceanography 28, 79–90. https://doi.org/10.1002/palo.20013.
van Hulten, M., Dutay, J.-C., Roy-Barman, M., 2018. A global scavenging and circulation ocean model of thorium-230 and protactinium-231 with improved particle dynamics (NEMO–ProThorP 0.1). Geosci. Model Dev. (GMD) 11, 3537–3556. https://doi.org/10.5194/gmd-11-3537-2018.
Waelbroeck, C., Pichat, S., Böhm, E., Lougheed, B.C., Faranda, D., Vrac, M., Missiaen, L., Vazquez Riveiros, N., Burckel, P., Lippold, J., Arz, H.W., Dokken, T., Thil, F., Dapoigny, A., 2018. Relative timing of precipitation and ocean circulation changes in the western equatorial Atlantic over the last 45 kyr. Clim. Past 14, 1315–1330. https://doi.org/10.5194/cp-14-1315-2018.
Walter, H.J., Van der Loeff, M.R., Hoeltzen, H., 1997. Enhanced scavenging of 231 Pa relative to 230 Th in the South Atlantic south of the Polar Front: implications for the use of the 231 Pa/230 Th ratio as a paleoproductivity proxy. Earth Planet Sci. Lett. 149, 85–100.
Yamamoto, A., Abe-Ouchi, A., Ohgaito, R., Ito, A., Oka, A., 2019. Glacial CO2 decrease and deep-water deoxygenation by iron fertilization from glaciogenic dust. Clim. Past 15, 981–996. https://doi.org/10.5194/cp-15-981-2019.